Electronic Supplementary Material (ESI) for Nanoscale Advances.

Supplementary Information

Revealing the Pulmonary Surfactant Corona on Silica Nanoparticles by Cryo-Transmission Electron Microscopy

F. Mousseau[a]*, E. Oikonomou[a], A. Vacher[b], M. Airiau[b], S. Mornet[c], J.-F. Berret[a]

[a] *Matière et Systèmes Complexes, UMR 7057 CNRS Université Denis Diderot Paris-VII, Bâtiment Condorcet, 10 rue Alice Domon et Léonie Duquet, 75205 Paris, France*
[b] *Solvay Research & Innovation Center Paris, 52 rue de la Haie Coq, 93306 Aubervilliers Cedex, France*
[d] *Institut de Chimie de la Matière Condensée de Bordeaux, UPR CNRS 9048, Université Bordeaux 1, 87 avenue du Docteur A. Schweitzer, Pessac cedex F-33608, France*

Outline

Corresponding author:
fanny.mousseau@univ-paris-diderot.fr

Supplementary Information S1 – Materials and Methods

1- Materials

Nanoparticles:
The positively charged silica particles were synthetized using the Stöber synthesis[1]. Briefly, fluorescent silica seeds were prepared in three steps. Rhodamine derivative "rhodamine red c2 maleimide" (Sigma Aldrich) was first covalently bound to the silica precursor (3-mercaptopropyl)-trimethoxysilane (MPS, Sigma Aldrich). The rhodamine–MPS compound was then mixed with a tetraethyl orthosilicate silica precursor (TEOS, Aldrich) and the Stöber synthesis was performed. With this approach the dyes were covalently bound to the silica matrix. In a third step, a non-fluorescent silica shell was grown with TEOS to increase the particle size and prevent leakage of the dyes out of the particles. Functionalization by amine groups was then performed, resulting in a positively charged coating[1]. Aminated silica was synthesized at 40 g L^{-1} and diluted with MilliQ-water at pH 5. The hydrodynamic and geometric diameters were determined as D_H = 60 nm and D_0 = 41.2 nm. The fluorescence properties were characterized using a Cary Eclipse fluorimeter (Agilent), with leading excitation and emission peaks at 572 nm and 590 nm, respectively. Negative silica particles (trade name CLX®) were purchased from Sigma Aldrich at the concentration of 450 g L^{-1}. The batch was diluted down to 50 g L^{-1} and dialyzed against MilliQ-water at pH 9 for two days. The diameters were measured at D_H = 34 nm and D_0 = 20 nm. For sake of simplification, the previous particles are abbreviated Silica (+) and Silica (-). Both of them are made of amorphous SiO_2.The surface charge density for the two particles was determined using the polyelectrolyte assisted charge titration spectrometry[2] at σ = +0.62 and -0.31e nm^{-2} respectively. Figure S1.1 shows the TEM images of the particles and Table S1.1 summarizes their bulk and surface properties.

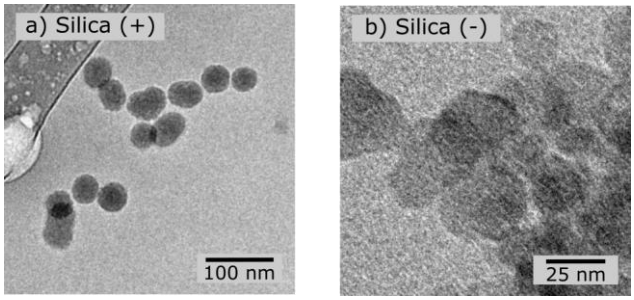

Figure S1.1: TEM images of positive (a) and negative (b) silica nanoparticles.

Nano-particle	Chemical composition	Function-nalization	D_0 (nm)	s	D_H (nm)	σ (nm^{-2})
Silica (+)	SiO_2	Amine	42	0.11	60	+0.62e
Silica (-)	SiO_2	/	20	0.20	34	-0.31e

Table S1.1: List of nanoparticles and their characteristics. D_0 and D_H stand for the geometric and hydrodynamic diameters determined by transmission electron microscopy and dynamic light scattering. s

denotes the size dispersity (ratio between the standard deviation and average size of the distribution) obtained by TEM. The electrostatic charge densities σ was obtained using polyelectrolyte assisted charge titration spectrometry[2].

Exogeneous pulmonary surfactant:
Curosurf®, also called Poractant Alfa (*Chiesi Pharmaceuticals*, Parma, Italy) is an extract of whole mince of porcine lung tissue purified by column chromatography. It is produced as a 80 g L^{-1} phospholipid and protein suspension containing among others phosphatidylcholine lipids, sphingomyelin, phosphatidylglycerol and the membrane proteins SP-B and SP-C[3]. The lipid and protein compositions of Curosurf® are provided in Table S1.2 and compared to that of native surfactant obtained by saline bronchoalveolar lavage[4]. Curosurf® is indicated for the rescue treatment of Respiratory Distress Syndrome (RDS) in premature infants and is administered at a dose of 200 mg per kilogram. It decreases their mortality up to 80%[5]. According to the manufacturer, the pH of Curosurf® is adjusted with sodium bicarbonate at pH 6.2[6]. Curosurf® was kindly provided by Dr. Mostafa Mokhtari and his team from the neonatal service at Hospital Kremlin-Bicêtre, Val-de-Marne, France.

Lipid composition (wt. % of total lipid)	**Native Surfactant**	**Curosurf®**
Phosphatidylcholine (PC)	70 - 85	67 - 74
Lysophosphatidyl choline (LPC)	0.5	< 1
Sphingomyelin	2	8.1
Cholesterol	5	0
Phosphatidylinositol (PI)	4 – 7	3.3
Phosphatidylserine (PS)	5	
Phosphatidylethanolamine (PE)	3	4.5
Phosphatidylglycerol (PG)	7 – 10	1.2
Protein concentration (wt. % of total lipid)	**Native Surfactant**	**Curosurf®**
SP-A	4	0
SP-B	1	0.3
SP-C	1	0.7
SP-D	4	0

Table S1.2: Lipid and protein compositions of native surfactant obtained by saline bronchoalveolar lavage compared to that of Curosurf®.

2- Methods

1) Cryo-transmission electron microscopy (cryo-TEM)

For cryogenic transmission electron microscopy (cryo-TEM), few microliters of surfactant (concentration 5 g L^{-1} in MilliQ-water) or silica–surfactant dispersions (see S1.6 for the concentrations) were deposited on a lacey carbon coated 200 mesh grid (Ted Pella Inc.). The drop

was blotted with a filter paper using a FEI VitrobotTM freeze plunger. The grid was then quenched rapidly in liquid ethane to avoid crystallization and later cooled with liquid nitrogen. It was then transferred into the vacuum column of a JEOL 1400 TEM microscope (120 kV) where it was maintained at liquid nitrogen temperature thanks to a cryo-holder (Gatan). The magnification was comprised between 3000× and 40000×, and images were recorded with an 2k×2k Ultrascan camera (Gatan). Images were digitized and treated by the ImageJ software and plugins (http://rsbweb.nih.gov/ij/).

2) Optical microscopy

Images were acquired on an IX73 inverted microscope (Olympus) equipped with an 60× objective. An EXi Blue camera (QImaging) and the Metaview software (Universal Imaging Inc.) were used as the acquisition system. The illumination system "Illuminateur XCite Microscope" produced a white light, filtered for observing a red (excitation filter at 545 nm - bandwidth 30 nm and emission filter at 620 nm - bandwidth 60 nm) or a green (excitation filter at 470 nm - bandwidth 40 nm and emission filter at 525 nm - bandwidth 50 nm) signal in fluorescence.
Glass slides were coated using polydiallyldimethylammonium chloride (PDADMAC, 26.8 kDa, Sigma Aldrich) to improve the surface adhesion of Curosurf® or of the NPs / Curosurf® mixtures. Thirty microliters of dispersion were deposited on a glass plate and sealed into a Gene Frame dual adhesive system (Abgene/ Advanced Biotech).
For experiments performed at 37 °C, samples and slides were previously equilibrated at physiological temperature for 15 min. During observation, the slide was placed in a chamber (Heating Insert P Lab-TekTM, PECON) thermostated at 37°C by the Tempcontrol 37-2 digital module (PECON). Images were digitized and treated by the ImageJ software and plugins (http://rsbweb.nih.gov/ij/).

3) Dynamic Light Scattering (DLS)

The scattered intensity I_S and the hydrodynamic diameter D_H were obtained from the NanoZS Zetasizer spectrometer (Malvern Instruments). The second-order autocorrelation function was analyzed using the cumulant and CONTIN algorithms to determine the average diffusion coefficient D_C of the scatterers. D_H was calculated according to the Stokes-Einstein relation $D_H = k_B T/3\pi\eta D_C$ where k_B is the Boltzmann constant, T the temperature and η the solvent viscosity. The hydrodynamic diameters provided here are the second coefficients in the cumulant analysis described as Z_{Ave}. Measurements were performed in triplicate at 25 °C after an equilibration time of 120 s.

4) Zeta potential

Laser Doppler velocimetry using the phase analysis light scattering mode and detection at an angle of 16° was used to carry out the electrokinetic measurements of electrophoretic mobility and zeta potential with the Zetasizer Nano ZS equipment (Malvern Instruments, UK). Zeta potential was measured after 120 s of equilibration at 25 °C.

5) Extrusion

Curosurf® extrusion was performed using an Avanti Mini Extruder (Avanti Polar Lipids, Inc. Alabama, USA). Solutions were prepared at 10 g L^{-1} and extruded 50 times at 37 °C through Whatman Nucleopor polycarbonate membranes (pore size of 100 nm). The extrusion device and membrane scission mechanism, as well as the results of the vesicular size are summarized in **Supplementary Information S4**.

6) Incubation of NPs with Curosurf®

To study the PS corona on silica particles, NPs / Curosurf® mixtures are prepared with an excess of Curosurf® to be close to the physiological conditions. Since the PS corona has been shown to be formed in less than 5 min[7], samples are kept 24 h at 37 °C to ensure the complete corona formation. Except specified otherwise, nanoparticles and pulmonary surfactant are not sonicated nor centrifugated prior or after mixing.

a. Silica (+) or (-) and Curosurf®

Equal volumes of silica particles and Curosurf® diluted in MilliQ-water at 0.45 and 10 g L^{-1} respectively were mixed at room temperature. The dispersion was kept 24 h at 37 °C before analysis. In the case of Silica (-), the pH of the diluted particles was adjusted to pH 6.4 with HCl before mixing with Curosurf®.

b. Silica (+) and extruded Curosurf®

Equal volumes of Silica (+) and extruded Curosurf® diluted in MilliQ-water at 0.4 and 4 g L^{-1} respectively were mixed at room temperature. The dispersion was kept 24 h at 37 °C before analysis.

c. Sonicated dispersion of Silica (+) and Curosurf®

Equal volumes of Silica (+) and extruded Curosurf® diluted in MilliQ-water at 6 and 4.26 g L^{-1} respectively were mixed at room temperature and sonicated during 90 min. Pertaining to the sonication, a sonicator bath (Bioblock Scientific, model 89202) working at the frequency of 35 kHz and an applied power of 55 W was used. During sonication, the temperature was maintained between 30 °C and 40 °C. The dispersion was diluted 10 times before observation with cryo-TEM.

7) Transmission electron microscopy (TEM)

Transmission electron microscopy (TEM) imaging was performed with a Tecnai 12 operating at 80 kV equipped with a 1k×1k Keen View camera. A 3 µL drop of Silica (+) / Curosurf® dispersion (concentration 0.1 g L^{-1}) was deposited on holey-carbon coated 300 mesh copper grids (Neyco). The sample was stained during 30 s with uranyl acetate at 0.5 wt. %. Uranyl acetate provides a dark labeling of the phospholipid heads due to the high affinity of the electron dense ion uranyl to carboxyl groups[8]. Grids were let to dry at room temperature in the dark for 20 min. Images were digitized and treated by the ImageJ software and plugins (http://rsbweb.nih.gov/ij/).

Supplementary Information S2 – Physico-chemical characterization of Curosurf®

The Curosurf® was characterized in terms of size distribution[9] (Figure S2.1), zeta potential (Figure S2.2) and melting temperature (Figure S2.3).

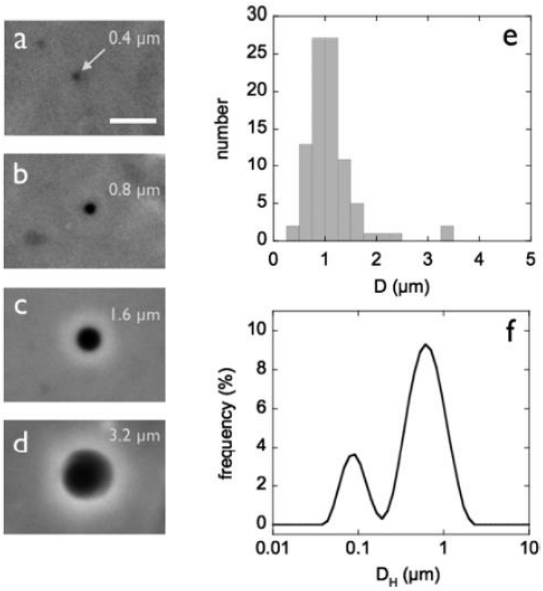

Figure S2.1: (a-d) Representative images of Curosurf® at the concentration of 0.1 g L^{-1} obtained by phase contrast optical microscopy at T = 25 °C (the bar is 3 µm). The sizes for the vesicles are indicated in the right-hand side of the panel. (e) Size distribution deduced from optical microscopy. An analysis of 100 objects resulted in a size distribution of median diameter 1.0 µm and standard deviation 0.5 µm (f) Distribution of hydrodynamic diameters of Curosurf® vesicles as determined by DLS. The size distribution is bimodal with two major peaks at 80 and 800 nm. On the one hand, the DLS peak at 800 nm is in agreement with the one found by microscopy. On the other hand, the DLS peak at 80 nm corresponds to a population of small vesicles that could not be detected by microscopy. Reprinted with permission from Langmuir (Mousseau *et al.*, Biophysicochemical Interaction of a Clinical Pulmonary Surfactant with Nanoalumina, 31, 7346–7354). Copyright 2015 American Chemical Society.

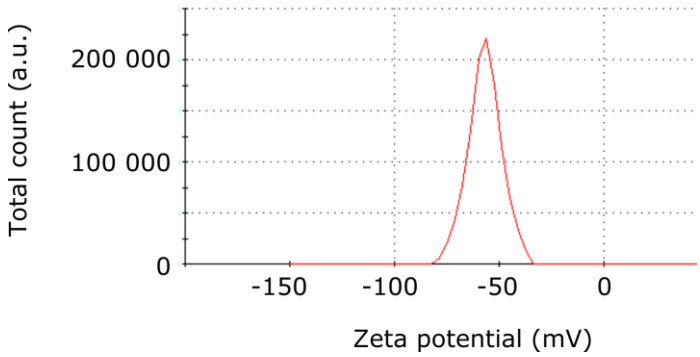

Figure S2.2: Zeta potential of Curosurf® diluted at 0.1 g L^{-1} in MilliQ-water. Results demonstrate that Curosurf® is negatively charged and has a zeta potential of – 55 mV.

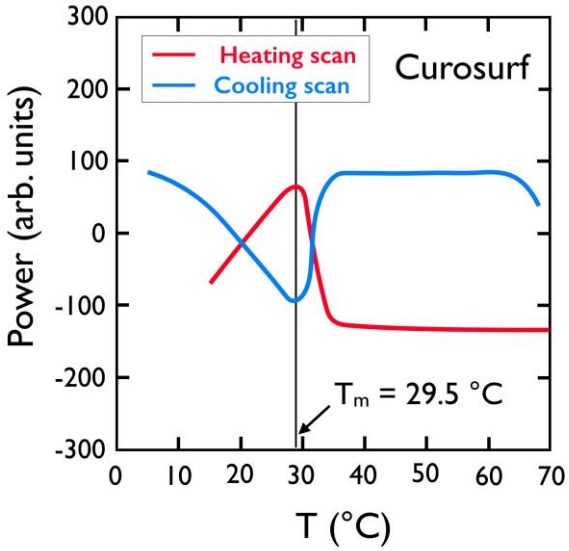

Figure S2.3: Thermograms of Curosurf® diluted in MilliQ-water at 10 g L^{-1} obtained by differential scanning calorimetry (DSC). The Curosurf® bilayer melting temperature was estimated at T_m = 29.5 °C from heating and cooling cycles. Thermograms were measured using an N-DSCIII instrument from CSC. The reference cell was filled with Milli-Q water and the sample cell (0.3 mL) with Curosurf®. The capillary cells were not capped and a constant pressure of 5×10^5 Pa was applied. The transition temperature was taken at the second, third and fourth heating scans, at a scan rate of 0.5 °C min^{-1} (from 5 to 70 °C). The melting temperature was estimated as the mean of the three transition temperatures mentioned before. The same procedure was applied with the cooling scans, which were performed in the same conditions.

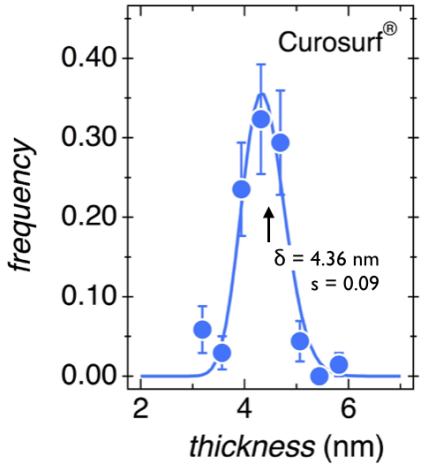

Figure S2.4: Distribution of Curosurf® membrane thickness obtained by cryo-TEM. The average value is δ = 4.36 nm. The distribution was determined on n = 68 measurements.

Supplementary Information Figure S3 – Study of Curosurf® corona at the micron scale

Here we address the issue of the structure at the micron scale of the PS corona on Silica (+) and Silica (-), following experiments performed previously on other nanoparticles[9,10].

1) Size distribution of nanoparticle-vesicle aggregates monitored by optical microscopy

Figure S3.1 shows phase-contrast optical microscopy images of Curosurf® or of NPs incubated in PS and on the right-hand side the corresponding size distributions. With Silica (+), large aggregates are visible and characterized by an average size of 3.7 µm, i.e. larger than Curosurf® vesicles (1.8 µm). Thus, incubation of Silica (+) in pulmonary surfactant leads to sample aggregation with agglomerates ranging from 2 to 20 µm. The data for silica (-) do not reveal the presence of micron-sized aggregates.

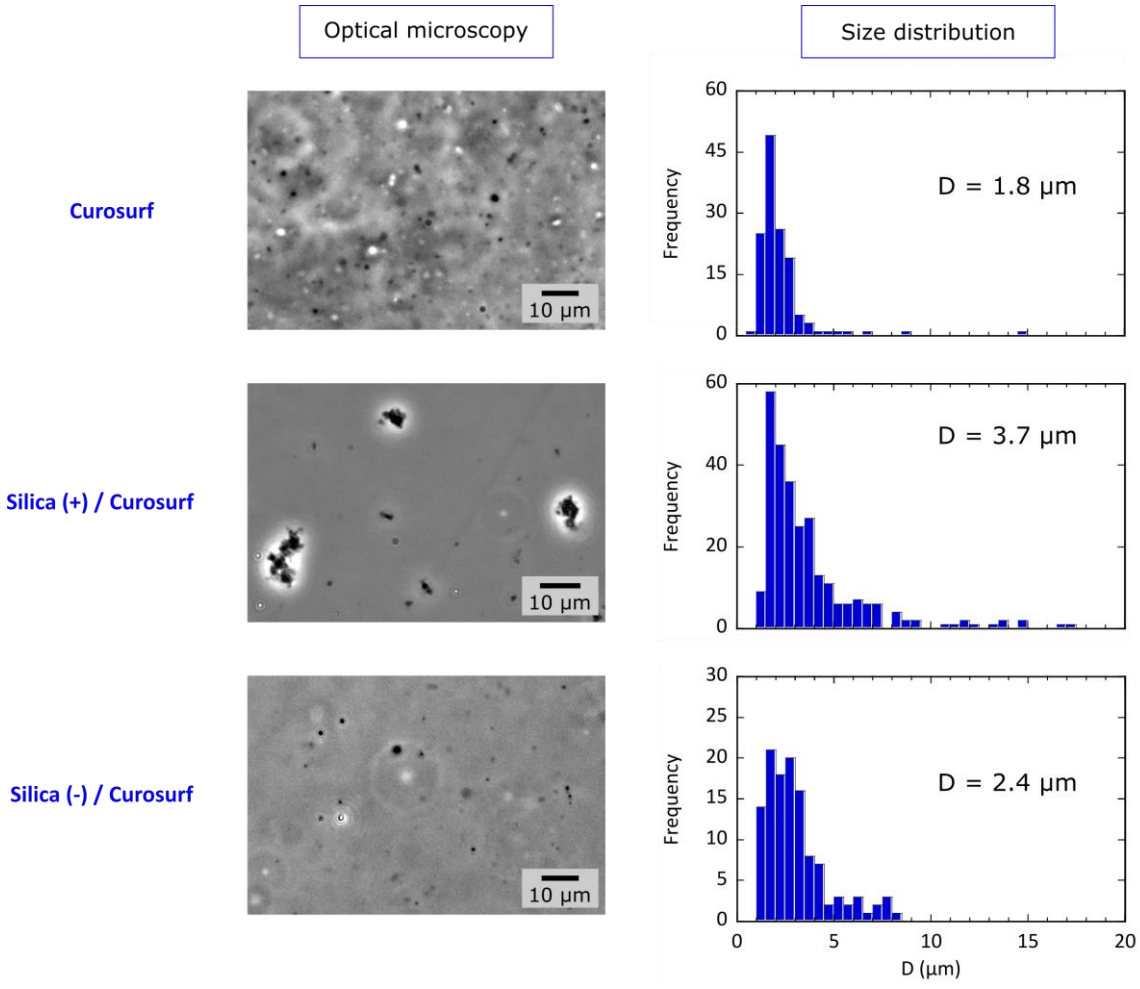

Figure S3.1: Right-hand side: phase-contrast optical microscopy images of Curosurf® and of mixed dispersions obtained from Silica (+) or Silica (-) and Curosurf®. The experimental conditions are c = 0.33 g L^{-1} for Curosurf® and c = 0.66 g L^{-1} for negative particles and c = 0.66 g L^{-1} for Curosurf® and c = 0.33 g L^{-1} for the positive ones. Images were performed at 25 °C. Left-hand side: size distribution derived from these and other microscopy images.

2) Fluorescence optical images of Silica (+) and fluorently labelled Curosurf®

To determine if the observed aggregates are made of vesicles, NPs or both, we take advantage of the optical properties of the Silica (+) that fluoresce in the orange-red at 590 nm. In parallel, the Curosurf® vesicles are labeled in green[11]. Figure S3.2-A presents an extended view of a Silica (+) / Curosurf® dispersion observed under phase contrast (a), green (b) and red (c) illumination. The merge image (d) of the green and red channels exhibits an excellent superimposition of the fluorescence, indicating that the aggregates contain both NPs and Curosurf®. The inner aggregate structure can be seen further at higher magnification (Figure S3.2-B). These results show that the aggregates are made of vesicles and particles and that both are intermixed at the micron scale.

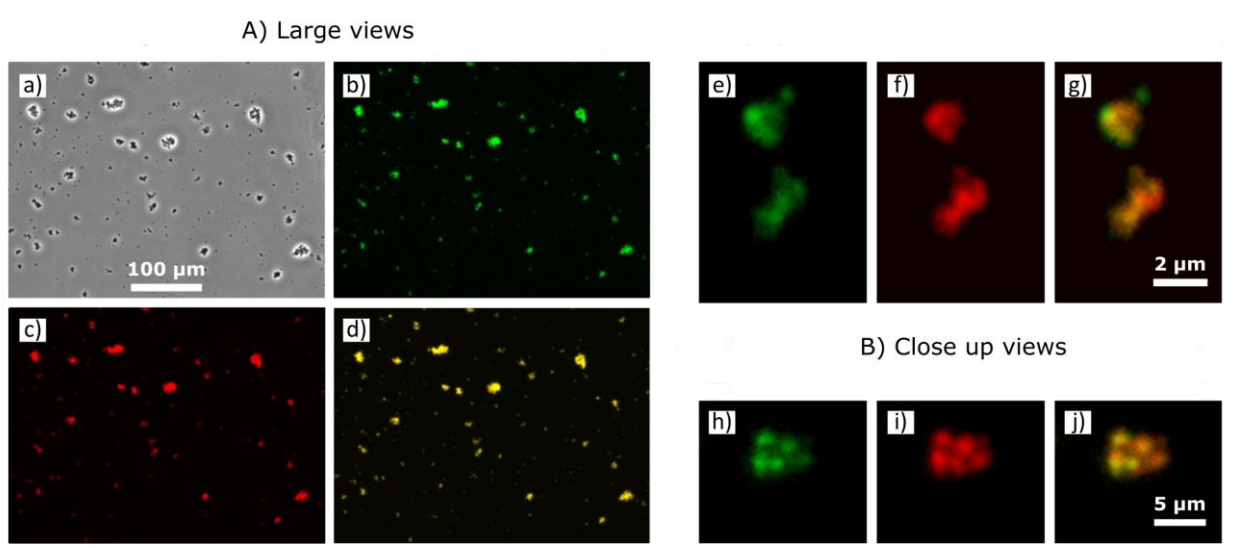

Figure S3.2: Close views of aggregates made from positive silica nanoparticles and Curosurf® observed by optical and fluorescence microscopy (magnification 60×). The experimental conditions are T = 37 °C , c = 0.66 g L^{-1} for Curosurf® and , c = 0.33 g L^{-1} for particles. The Silica (+) are synthesized to fluoresce in the orange-red at 590 nm and the vesicles are labeled with a green fluorescent lipid (PKH67) emitting at 502 nm. The aggregates are observed under phase contrast (a), green (b, e, h) and red (c, f, i) illumination. The merge signals are shown in (d, g, j).

3) TEM images of Silica (+) incubated in Curosurf®

To have a better idea of the aggregates structure, TEM was performed on Silica (+) incubated in Curosurf®. Figure S3.3 displays images of 4 agglomerates. On the one hand, NPs (blue arrows) and intact PS vesicles (red arrows) are shown to interact together (images a and b). On the other hand, aggregated particles are observed (image c). A close view (image d) illustrates that aggregated NPs are either naked or coated by phospholipids (yellow arrows). A schematic representation of these two corona structures is depicted in Figure S3.3-e. These results are in agreement with the one obtained when positive aluminum oxide nanoparticles are incubated in Curosurf® [9].

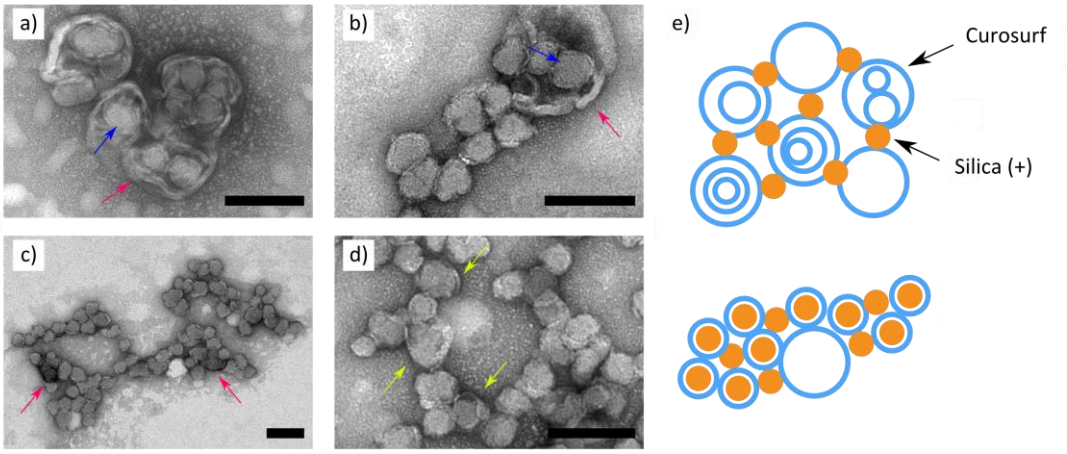

Figure S3.3: a-d) Aggregates made from positive silica nanoparticles and Curosurf® observed by TEM at 0.1 g L^{-1}. Scale bars: 100 nm. e) Schematic representations of the different hybrid structures observed on TEM images.

4) Conclusion

Incubation of silica particles with pulmonary surfactant give rise to different assemblies at the micron scale, depending on the NP charge. In the particular case of Silica (+), hybrid NPs / vesicles aggregates are formed. Although the PS corona structure determination is limited by the spatial resolution of optical microscopy and classical TEM, our results undeniably demonstrate that the PS corona on nanoparticles can't be reduced to supported lipid bilayers.

Supplementary Information S4 – Additional cryo-TEM images of silica nanoparticles incubated with Curosurf®

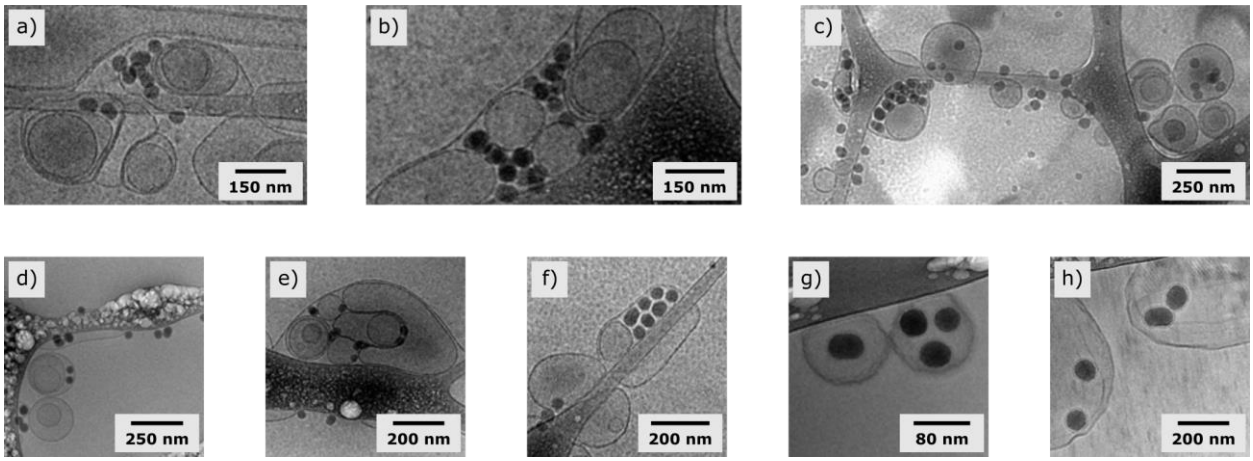

Figure S4.1: Cryo-TEM pictures of Silica (+) incubated in Curosurf®.

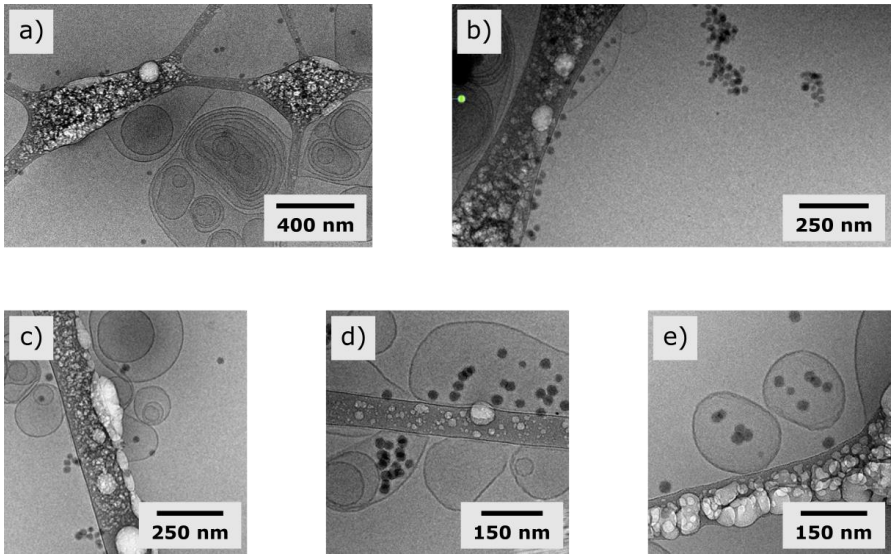

Figure S4.2: Cryo-TEM pictures of Silica (-) incubated in Curosurf®.

Supplementary Information S5 – Curosurf® extrusion

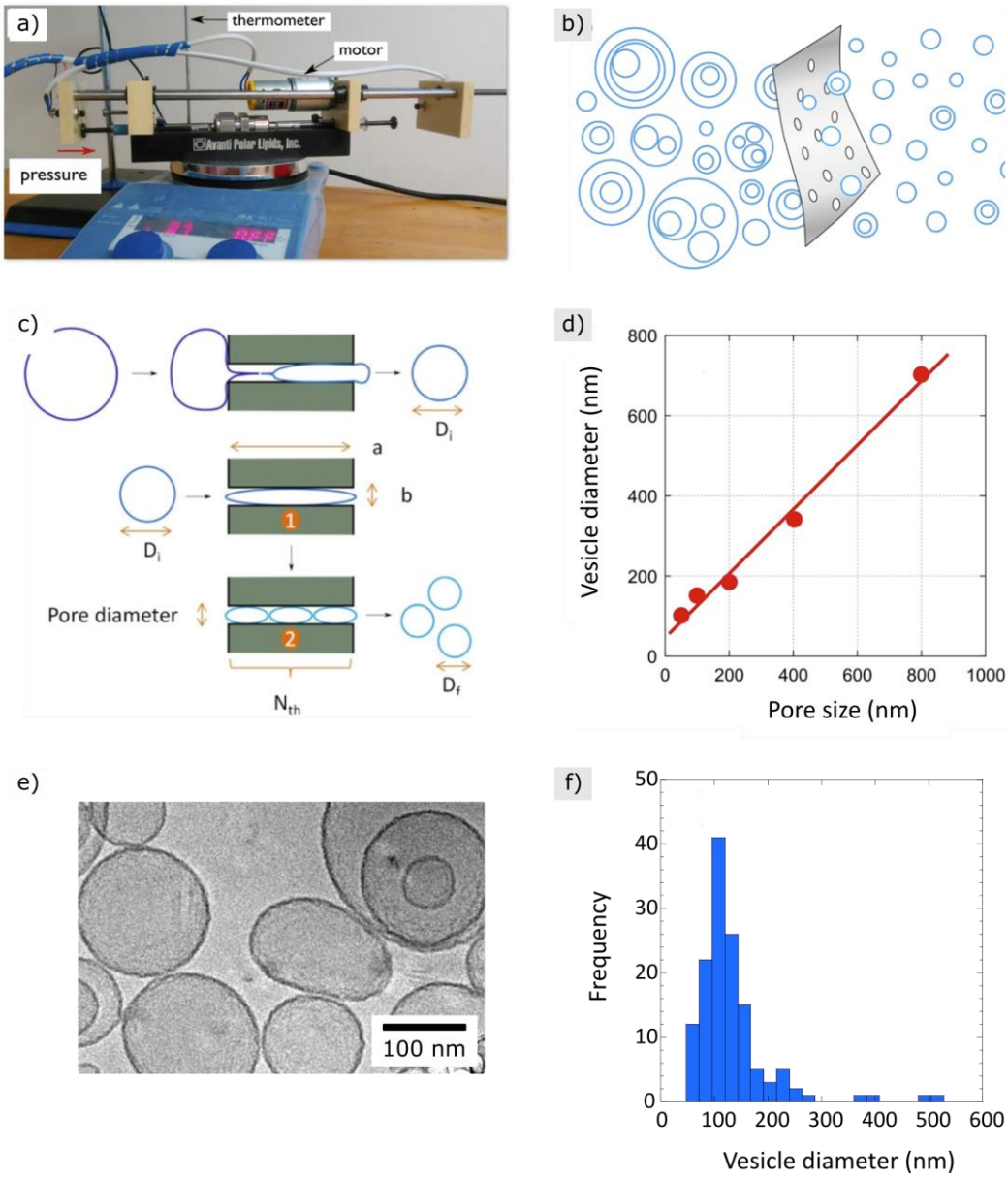

Figure S5.1: a) Device used for extruding phospholipid dispersions using polycarbonate filter with controlled pore size. b) Schematic illustration of the extrusion process. c) Modeling the extrusion process: A two-steps model was developed to describe the extrusion of Curosurf® [9]. This model assumes that in the first passages, micron size vesicles are blocked at the pore entries, causing strong deformation and membrane breakings. For later passages, the vesicles are sheared and stretched in the pores, leading to a Rayleigh-like instability, and causing multilamellar vesicles fragmentation into objects of diameter of the order of the pore size. d) Vesicle size dependence as a function of the pore size. The sizes were obtained from dynamic light scattering. e) Cryo-TEM images of Curosurf® extruded with pores of 100 nm and diluted in MilliQ-water at 4 g L^{-1}. f) Size distribution of extruded vesicles obtained from cryo-TEM images of Curosurf® extruded with pores of 100 nm. The measure of 136 vesicles gives D_0 = 132 ± 70 nm.

References

1. Reinhardt, N., Adumeau, L., Lambert, O., Ravaine, S. & Mornet, S. Quaternary ammonium groups exposed at the surface of silica nanoparticles suitable for DNA complexation in the presence of cationic lipids. *J. Phys. Chem. B* **119**, 6401–6411 (2015).
2. Mousseau, F., Vitorazi, L., Herrmann, L., Mornet, S. & Berret, J.-F. Polyelectrolyte assisted charge titration spectrometry: Applications to latex and oxide nanoparticles. *J. Colloid Interface Sci.* **475**, 36–45 (2016).
3. www.curosurf.com, consulté le 02.10.16.
4. Braun, A. *et al.* A Freeze-Fracture Transmission Electron Microscopy and Small Angle X-Ray Diffraction Study of the Effects of Albumin, Serum, and Polymers on Clinical Lung Surfactant Microstructure. *Biophys. J.* **93**, 123–139 (2007).
5. Lopez-Rodriguez, E. & Pérez-Gil, J. Structure-function relationships in pulmonary surfactant membranes: From biophysics to therapy. *Biochim. Biophys. Acta BBA - Biomembr.* **1838**, 1568–1585 (2014).
6. Minkov, I., Mircheva, K., Grozev, N., Ivanova, Tz. & Panaiotov, I. Properties of mixed monolayers of clinical lung surfactant, serum albumin and hydrophilic polymers. *Colloids Surf. B Biointerfaces* **101**, 135–142 (2013).
7. Kumar, A. *et al.* Enrichment of immunoregulatory proteins in the biomolecular corona of nanoparticles within human respiratory tract lining fluid. *Nanomedicine Nanotechnol. Biol. Med.* **12**, 1033–1043 (2016).
8. Hayat, M. A. Principles and techniques of electron microscopy: Biological applications. in *Principles and techniques of electron microscopy: Biological applications* **4th ed**, 545 (2000).
9. Mousseau, F., Le Borgne, R., Seyrek, E. & Berret, J.-F. Biophysicochemical Interaction of a Clinical Pulmonary Surfactant with Nanoalumina. *Langmuir* **31**, 7346–7354 (2015).
10. Mousseau, F. & Berret, J.-F. The role of surface charge in the interaction of nanoparticles with model pulmonary surfactants. *Soft Matter* **14**, 5764–5774 (2018).
11. Mousseau, F., Berret, J.-F. & Oikonomou, E. K. Design and Applications of a Fluorescent Labeling Technique for Lipid and Surfactant Preformed Vesicles. *ACS Omega* **4**, 10485–10493 (2019).